

Electrodeposition of palladium–indium from 1-ethyl-3-methylimidazolium chloride tetrafluoroborate ionic liquid

Shu-I Hsiu, Chia-Cheng Tai, I-Wen Sun*

Department of Chemistry, National Cheng Kung University, Tainan, Taiwan, ROC

Received 6 April 2005; received in revised form 27 July 2005; accepted 30 July 2005

Available online 6 September 2005

Abstract

Voltammetry at a glassy carbon electrode was used to study the electrochemical co-deposition of Pd–In from a chloride-rich 1-ethyl-3-methylimidazolium chloride/tetrafluoroborate air-stable room temperature ionic liquid at 120 °C. Deposition of Pd alone occurs prior to the overpotential deposition (OPD) of bulk In. However, underpotential deposition (UPD) of In on the deposited Pd was observed at the potential same as the deposition of Pd. The UPD of In on Pd was, however, limited by a slow charge transfer rate. Samples of Pd–In alloy coatings were prepared on nickel substrates and characterized by energy dispersive spectroscopy (EDS), scanning electron microscope (SEM) and X-ray powder diffraction (XRD). The electrodeposited alloy composition was relatively independent on the deposition potential within the In UPD range. At more negative potentials where the OPD of Pd–In has reached mass-transport limited region, the alloy composition corresponds to the Pd(II)/In(III) composition in the plating bath. The Pd–In alloy coatings obtained by direct deposition of Pd and UPD of In on the deposited Pd appeared to be superior to the Pd–In alloys that were obtained via the co-deposition of Pd and bulk In at OPD potentials.

© 2005 Elsevier Ltd. All rights reserved.

Keywords: Electrodeposition; Ionic liquid; Pd–In; Molten salt

1. Introduction

Electrodeposition of palladium–indium alloys is of interest [1] because the incorporation of indium into palladium provides higher microhardness and wear-resistance than pure palladium without sacrificing the low contact resistance of the palladium. Thus, the Pd–In coatings can be used as replacement for pure gold, silver and palladium coatings in various applications. Many examples of the electrodeposition of Pd–In in aqueous baths are available nowadays [2–6]. The general difficulties associated with the electrodeposition of Pd–In from aqueous baths are the considerable difference between the deposition potentials of palladium and indium, the low hydrogen overvoltage and the large hydrogen solubility in the Pd metal. Therefore, efforts have been made to minimize these problems. One approach is to replace the aqueous baths with aprotic solvents.

Over the past 2 decades, room temperature ionic liquids (ILs) have been drawing considerable interest as media in the area of electrochemical processes [7–14], organic synthesis [15–18], catalysis [19–21] and chemical separation [22–24]. For electrochemical applications, ILs exhibit several advantages over the conventional molecular solvent including good electrical conductivity, wide electrochemical window, low vapor pressure and good thermal stability. Moreover, ILs are in most cases aprotic so that complications associated with hydrogen evolution that occur in aqueous electrolytes are excluded. Thus, ionic liquids have been employed in the electrodeposition of pure metals and alloys, especially those that are difficult to prepare in aqueous electrolytes. Generally, ILs can be classified into water/air sensitive and water/air stable. The water/air stable ILs are more versatile to work with. Until now, studies of the electrodeposition of some metals, metal alloys and semiconductors in the water/air stable ILs have been reported [25–30], but the electrochemical investigation of palladium and its alloys in ILs are very limited [31–33]. In view of the difference between aqueous

* Corresponding author.

E-mail address: iwsun@mail.ncku.edu.tw (I.-W. Sun).

solutions and ILs, it is meaningful to accumulate fundamental data of the electrochemical investigation of Pd–In alloy in the ionic liquids. In this study, the electrodeposition of Pd–In was investigated in a hydrophilic water-stable Lewis basic 1-ethyl-3-methylimidazolium chloride-tetrafluoroborate ([EMIm]Cl-BF₄) IL that contained excess amounts of chloride ions. The electrochemical reduction of Pd and In was studied with cyclic voltammetry at 120 °C. Thin films of Pd–In alloys were electrodeposited with constant potential electrolysis at nickel substrates and characterized. The effects of deposition potential and plating concentrations on the composition and morphology of the electrodeposits were examined.

2. Experimental

2.1. Apparatus

All electrochemical experiments were conducted in a N₂-filled glove-box system (Vacuum Atmosphere Co.) in which the moisture and oxygen contents were kept below 1 ppm. The electrochemical experiments were accomplished by an EG&G Princeton Applied Research Corporation (PAR) model 273A potentiostat controlled by EG&G PAR model 270 software. A three-electrode cell was used for the electrochemical experiments. For static voltammetry, the working electrode was a glassy carbon (GC) disk electrode ($A = 0.07 \text{ cm}^2$). The counter electrode was an aluminum (Aldrich, 99.99%) spiral immersed in the pure [EMIm]Cl-BF₄ IL contained in a glass tube having a fine porosity tip. The reference electrode was an aluminum wire immersed in a 60–40 mol% AlCl₃-[EMIm]Cl ionic liquid contained in the same type of glass tube as the counter electrode. A Pine model AFMSR electrode rotator was employed for rotating disk electrode voltammetry. Electrodeposition experiments were conducted on nickel plates (Aldrich, 99.99%). A Hitachi S-4200 field emission scanning electron microscope (SEM) with an energy dispersive spectroscope (EDS) working at 15 kV was used to examine the surface morphology of the electrodeposits. The crystalline phases of the deposits were studied with a Shimadzu XD-D1 X-ray diffractometer (XRD).

2.2. Chemicals

1-Ethyl-3-methylimidazolium chloride was prepared and purified according to literature [34]. Sodium tetrafluoroborate (Aldrich, 98%), anhydrous PdCl₂ (Aldrich, 99.9%), anhydrous InCl₃ (Stream, 99.99%) were used as received. The [EMIm]Cl-BF₄ ionic liquid was prepared by direct reaction of proper amounts of [EMIm]Cl and NaBF₄ in acetone as described previously [25]. The ionic liquid used in this study contains 0.80 M chloride, which was introduced by dissolution of [EMIm]Cl.

3. Results and discussion

3.1. Voltammetric behavior

Both PdCl₂ and InCl₃ dissolve readily in the basic [EMIm]Cl-BF₄ ILs. Previous literature indicated that Pd(II) and In(III) exist as the [PdCl₄]²⁻ and [InCl₅]²⁻ complex anions, respectively, in chloride-rich chloroaluminate ILs [31,35]. A typical cyclic voltammogram recorded at a glassy carbon electrode for 10 mM Pd(II) in the basic [EMIm]Cl-BF₄ IL at 120 °C is shown in Fig. 1a. The reduction of Pd(II) occurs at the cathodic wave c₁ and the oxidation of the electrodeposited Pd occurs at the anodic wave a₁. A typical cyclic voltammogram of 20 mM In(III) at a glassy carbon electrode in the basic [EMIm]Cl-BF₄ IL at 120 °C is presented in Fig. 1b. This cyclic voltammogram reveals that the electrodeposition of In (wave c₂) occurs at a potential far more negative than the deposition of the Pd. The considerable difference between the deposition potentials of the individual component implies that electrodeposition of compact Pd–In alloys may be difficult. On the anodic scan, Fig. 1b shows a sharp wave, a₂, due to the stripping of the bulk indium deposits and a small broad anodic wave at about –0.3 V which may be due to the stripping of the In deposits having stronger interactions with the GC substrate. Fig. 1c shows the cyclic voltammogram of a solution containing 10 mM Pd(II) and 20 mM In(III) in the basic [EMIm]Cl-BF₄ IL at 120 °C. As can be seen in this voltammogram, the deposition of In and Pd both shift negatively in comparison to the deposition of individual metals shown in Fig. 1a and b. On the

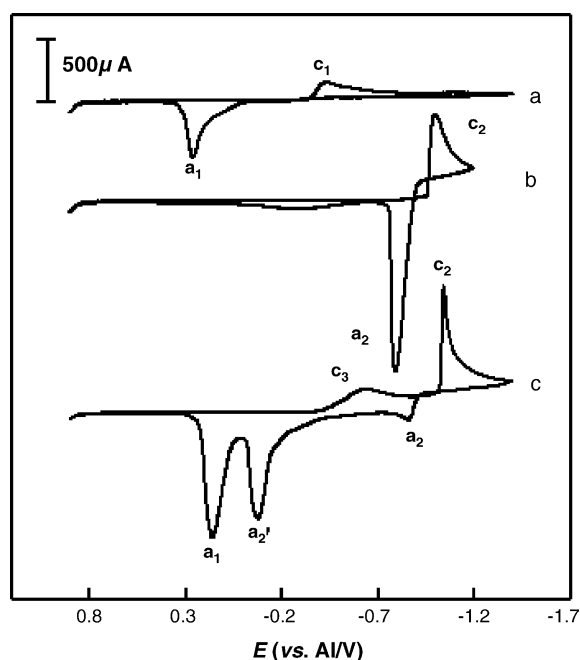


Fig. 1. Cyclic voltammograms of (a) 10 mM Pd(II), (b) 20 mM In(III) and (c) 10 mM Pd(II) + 20 mM In(III) in a [EMIm]Cl-BF₄ ionic liquid at a GC electrode at 120 °C. Scan rate = 100 mV s⁻¹.

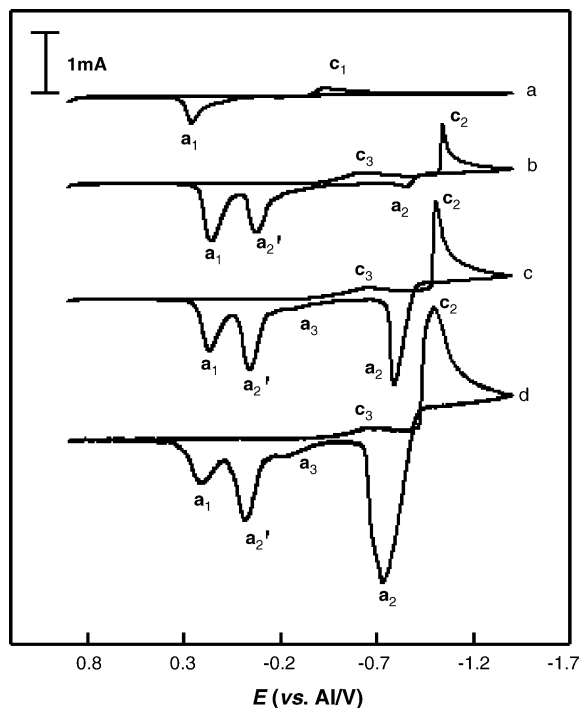


Fig. 2. Cyclic voltammograms of 10 mM Pd(II) and (a) 0, (b) 20, (c) 40 and (d) 80 mM In(III) in a [EMIm]Cl-BF₄ ionic liquid at a GC electrode at 120 °C. Scan rate = 100 mV s⁻¹.

anodic potential scan, the anodic wave a_2 for the stripping of bulk In deposits decreases significantly while a new wave a'_2 becomes apparent. Furthermore, the anodic wave a_1 for the stripping of bulk Pd shifts to a less positive potential and its peak current is significantly larger than that is observed in Fig. 1a. These changes in the voltammetric features strongly indicate the formation of Pd–In alloy. The multiple stripping peaks indicate the presence of different alloys phases. Based on their potentials, one would expect that a'_2 alloy to have a higher In concentration than the alloy stripped at a_1 . To further study the co-deposition of Pd–In, cyclic voltammograms were collected also for solutions containing 10 mM of Pd(II) and different concentrations of In(III). As shown in Fig. 2, wave a_1 increases when In(III) concentration is increased from 0 to 20 mM. Further increasing In(III) concentration, however, enhances waves c_2 , a_2 , a'_2 and a_3 but diminishes wave a_1 . Initially, at low In(III) concentration, the incorporation of In deposits into the Pd deposit increases the stripping current of wave a_1 (Figs. 2b) because three electrons are associated with each In atom and only two electrons are associated with one Pd atom. Fig. 2c and d indicates that further increasing the In(III) concentration increases the amount of the indium in the deposits which favors the formation of the alloy having higher In content and thus enhances wave a'_2 and diminishes wave a_1 which is due to the alloy having lower In content. It is noted that wave a_2 also increases with increasing In(III) because more of the excess In deposits remain as the bulk In deposits that do not interact effectively with Pd.

It is known that underpotential deposition (UPD) can occur when the work function of the deposited metal, ϕ_M , is fairly smaller than that of the substrate metal, ϕ_S . The underpotential shift, ΔE_p , has been found to vary linearly with the difference of work functions, $\Delta\phi$, according to the empirical expression: [36] $\Delta E_p = 0.5 \Delta\phi$. However, the presence of specific interactions between the deposit and the substrate can deviate this relationship. Considering the smaller work function of indium ($\phi_{In} = 4.12$ eV) with respect to the work function of palladium ($\phi_{Pd} = 5.12$ eV) [36], UPD of In on Pd is expected to occur at about -0.5 V. To see if the UPD of In on Pd indeed occurs, cyclic voltammograms of In(III) at the Pd electrode were recorded. A typical cyclic voltammogram of 20 mM In(III) recorded at a Pd wire electrode in the IL at 120 °C is shown in Fig. 3a. This figure reveals that, similar to that was observed in Fig. 1c, the OPD of In (wave c_2) at the Pd electrode occurs at a potential more negative than that was observed at a GC electrode (Fig. 1b), indicating a larger overpotential is required for the OPD of In at Pd. Fig. 3a also shows a small reduction wave c_3 at ca. -0.5 V, which does not occur at the GC electrode, prior to the bulk deposition of In and two anodic waves, a_3 and a'_3 in addition to wave a'_2 during the reverse scan. Because wave c_3 occurs at a potential positive to the potential for bulk deposition of In, it must be the UPD of In on Pd. To further study this behavior, the potential scan was held at wave c_3 for different periods of time before scanning in the reverse direction. As shown in Fig. 3b, prolonging the deposition time at wave c_3 does not increase significantly the anodic current (or the accumulated charge) of wave a_3 , indicating that the deposition of In at wave c_3 is a surface confined process, which is typical for a UPD behavior. Because the polycrystalline Pd electrode is used, the In UPD wave c_3 is broad. It is worthy to perform in the future experiments on Pd single crystals in order to have a more comprehensive understanding on the In UPD behavior. Fig. 3c compares the cyclic voltammograms of a Pd(II) solution and solutions containing fixed amount of Pd(II) and various amounts of In(III) recorded at a GC electrode. As can be seen, the presence of In(III) shifts the reduction of Pd(II) and the stripping of the deposited Pd to more negative potentials. The appearing of the alloy stripping waves (a_3 and a'_3) in addition to wave a_1 indicates that wave c_3 is resulting from the deposition of Pd and the UPD of In. Furthermore, increasing the In(III) concentration in the plating bath raises the anodic waves a_3 and a'_3 but suppresses wave a_1 . These results also suggest the alloying of the deposited Pd with the UPD In. Note that the anodic stripping wave a'_2 observed in Fig. 2 is not seen in this figure, suggesting that wave a'_2 is related to the alloys of Pd with OPD In whereas a_3 and a'_3 are related to the alloys of Pd with UPD In.

In addition to the cyclic voltammetric experiments on glassy carbon disc electrode, rotating disk electrode cyclic voltammetry (RDECV) was employed to study the electrodeposition of Pd and In. Because the glassy carbon RDE used in this study is stable only at temperatures below 80 °C, the experiments were conducted at 70 °C. Some typical GCRDE

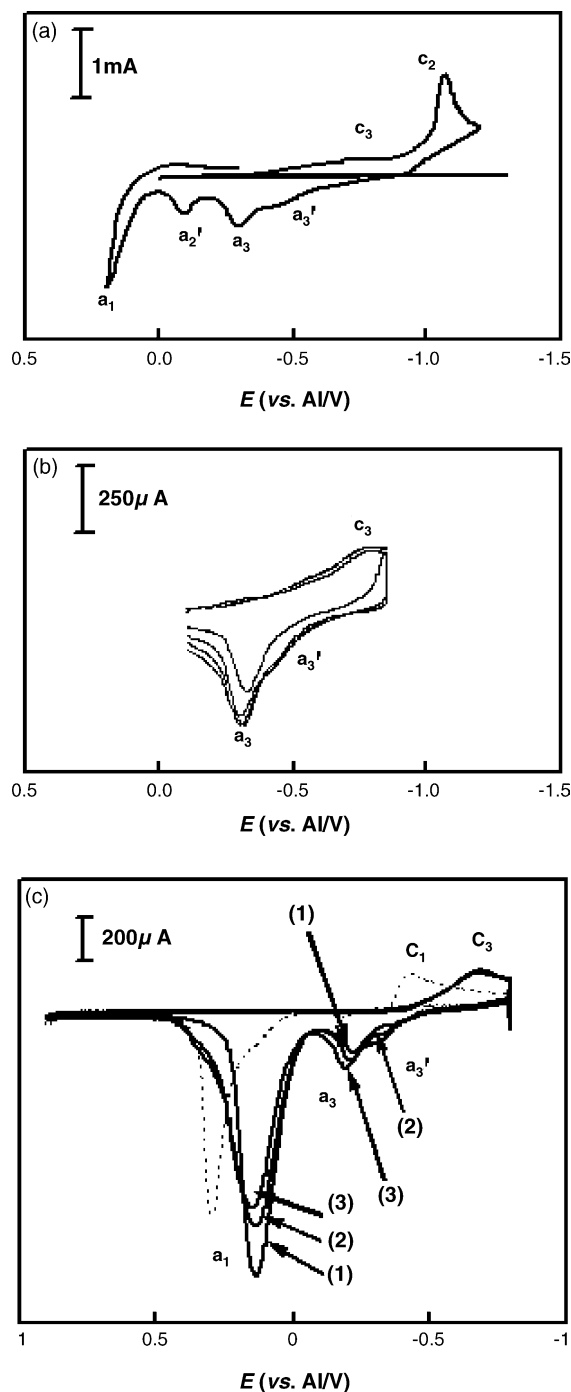


Fig. 3. Cyclic voltammograms of: (a) 20 mM In(III) IL solution recorded on a Pd electrode, (b) 20 mM In(III) IL solution recorded on a Pd electrode with potential scan was held at -0.85 V for 0, 20, 60, 100 and 140 s before reverse scan and (c) (---) 10 mM Pd(II) and 10 mM Pd plus (1) 40, (2) 60 and (3) 80 mM In(III) recorded on a GC electrode at 120 °C. Scan rate = 100 mV s^{-1} .

cyclic voltammograms are shown in Fig. 4. Fig. 4a and b are the voltammograms of a 20 mM In(III) solution and a 10 mM Pd(II) solution, respectively. From the concentrations of In(III) and Pd(II) and their limiting currents it is realized that the diffusion coefficient of Pd(II) is about the same as that of In(III). From separate chronoamperometry experiments, it

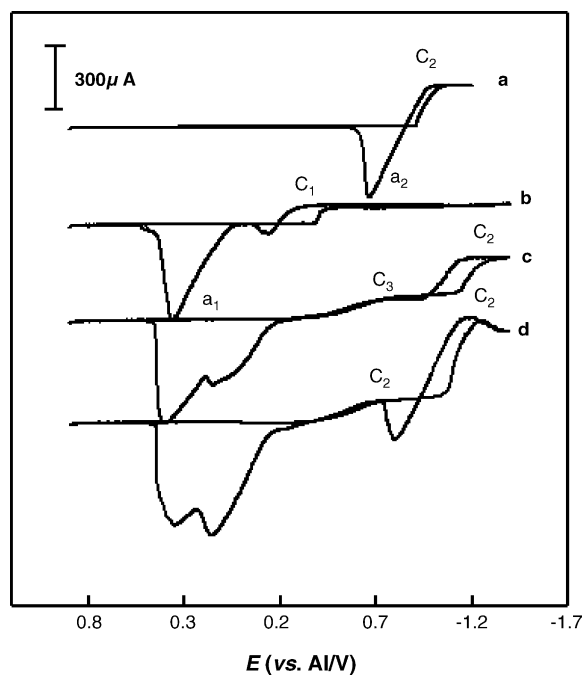


Fig. 4. Rotating disc electrode linear scan voltammograms of: (a) 20 mM In(III), (b) 10 mM Pd(II), (c) 10 mM Pd(II) and 20 mM In(III) and (d) 10 mM Pd(II) and 40 mM In(III) in a [EMIm]Cl- BF_4 ionic liquid at a GCRDE at 70 °C. Scan rate = 5 mV s^{-1} .

was estimated that the diffusion coefficients of In(III) and Pd(II) are 4.92×10^{-7} and 5.25×10^{-7} cm^2/s , respectively. Fig. 4c is the voltammogram of a IL containing 10 mM Pd(II) and 20 mM In(III). This voltammogram shows that both of the Pd(II) and In(III) reductions shifted to more negative potentials compared to Fig. 4a and b. Almost no anodic stripping (a_2) peak due to the OPD In deposits is seen in this voltammogram, suggesting that all the deposited In has alloyed with Pd. Fig. 4d shows that when the In(III) concentration was increased to 40 mM, the limiting current due to the OPD bulk In (wave c_2) increased and its corresponding anodic stripping wave a_2 became apparent, indicating that the In deposits did not alloy completely with Pd. It is also noted that increasing the In(III) concentration does not enhance wave c_3 , which is due to the bulk deposition of Pd and UPD of In, indicating that the UPD of In must have proceeded with a fairly slower rate in comparison to the deposition of Pd.

3.2. Bulk electrodeposition of Pd–In

Pd–In electrodeposits were prepared using constant potential electrolysis on nickel foils (0.5×0.5 cm^2) in [EMIm]Cl- BF_4 IL containing Pd(II) and In(III). Following each deposition experiment, the Pd–In-coated foil was immersed in a small volume of blank ionic liquid and transferred out of the glove box to be rinsed with deionized water to remove any residual ionic liquid. The electrodeposits were characterized by SEM, EDS and XRD analysis.

The compositions of the electrodeposits that were prepared at 120 °C are plotted in Fig. 5 as a function of deposition

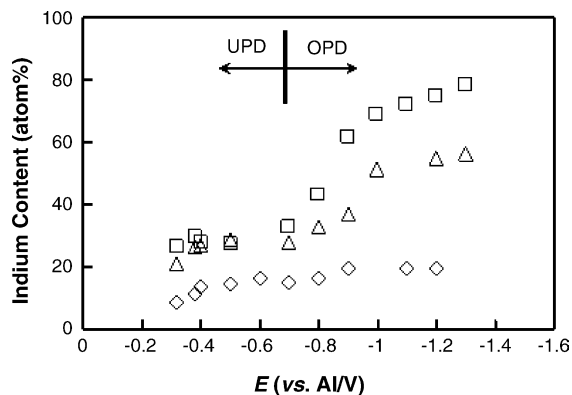


Fig. 5. Variation of the Pd–In electrodeposit composition with deposition potential. The deposits were prepared in a [EMIm]Cl-BF₄ ionic liquid at 120 °C containing: (Δ) 10 mM Pd(II) and 10 mM In(III); (\square) 10 mM Pd(II) and 40 mM In(III); (\diamond) 40 mM Pd(II) and 10 mM In(III).

potential. In general, the In composition (a/o) in the deposit increases slowly as the deposition potential changes from -0.3 to -0.7 V, which is the potential region for the UPD of In on Pd. As the deposition potential becomes more negative than -0.7 V, where OPD of In takes place, the In content in the deposits increased rapidly until the deposition potential reached the region where OPD of In was mass-transport limited. When the deposition was conducted within the In UPD potential range, the deposits composition did not change significantly with increasing In(III) concentration if the Pd(II)

concentration in the plating solution was kept constant. On the other hand, when the concentration of In(III) in the plating bath was kept constant, the In content lowered with increasing Pd(II) concentration. These results suggest that the In UPD rate was slower than the deposition rate of Pd.

In the potential range ($E < -0.7$ V) where OPD of In occurred, the In content in the deposits increased with increasing In(III) concentration. When the potential reached the mass-transport-limited region, the electrodeposits composition ratio approximated the Pd(II)/In(III) concentration ratio in the plating solution in consistent with the fact that the diffusion coefficients of Pd(II) and In(III) are about the same.

The morphologies of the electrodeposits obtained at different deposition potentials are illustrated in Fig. 6. These micrographs show that the electrodeposits prepared within the potential region of the simultaneous deposition of Pd and UPD of In consist uniformly distributed nodules which grow in size with increasing deposition overpotential due to the increased deposition rate. As the deposition potential is changed to more negative value where OPD of bulk In also occurs, dendrite morphologies become apparent, suggesting that the deposits are not homogenous but mixtures of Pd, In and Pd–In alloys. Minor cracks appear in some of the deposits. These cracks may result from the entrained ionic liquid as indicated by EDS analysis which showed the presence of traces Cl in these deposits. Typical XRD patterns of Pd–In films prepared at 120 °C from [EMIm]Cl-BF₄ contain-

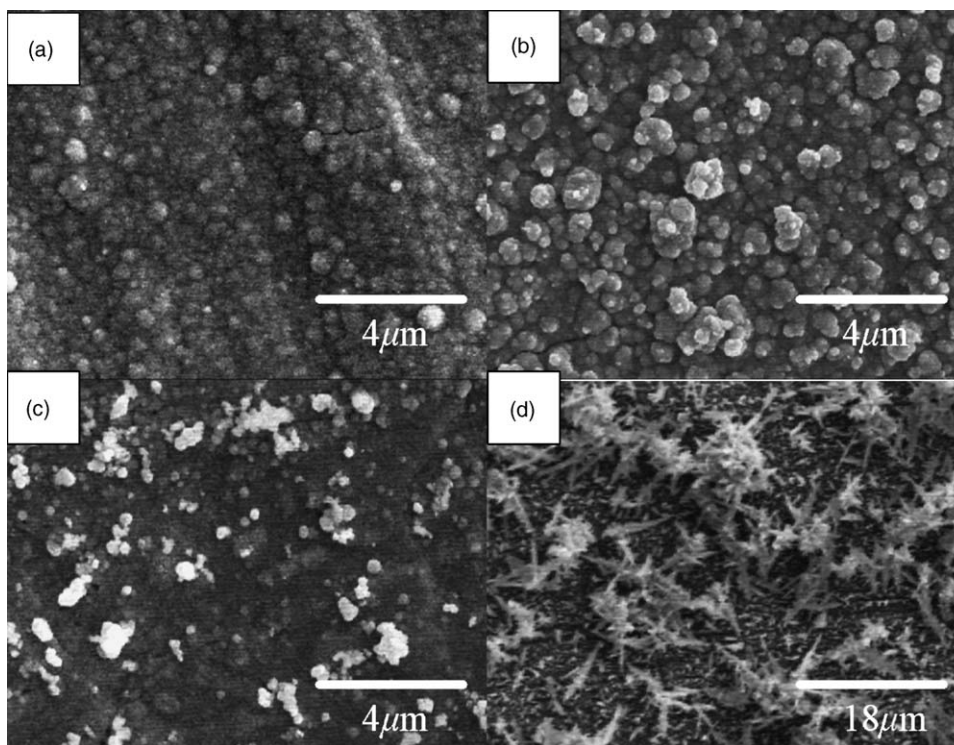


Fig. 6. SEM micrographs of Pd–In electrodeposits prepared on nickel substrates from a [EMIm]Cl-BF₄ ionic liquid solution containing 10 mM Pd and 20 mM In(III) at 120 °C. The depositional potential and the Pd content (a/o), respectively, in the deposits are: (a) -0.28 V, 73 a/o; (b) -0.5 V, 74 a/o; (c) -0.7 V, 67 a/o; (d) -1.0 V, 36 a/o.

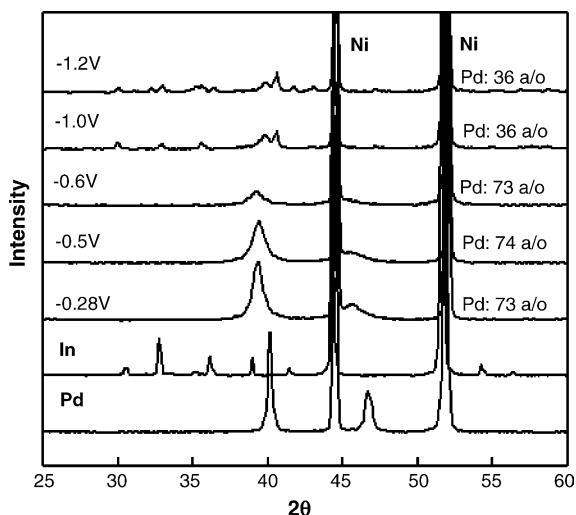


Fig. 7. XRD patterns (Cu $K\alpha$) of Pd–In sample prepared on nickel substrate from [EMIm]Cl- BF_4 ionic liquid containing 10 mM Pd(II) and 20 mM In(III) at 120 °C.

ing 10 mM In(III) and 20 mM Pd(II) at different potentials are shown in Fig. 7. For comparison, XRD patterns of pure Pd and In deposits are also presented in this figure.

For the deposits having a high Pd content (73 at.%), which were prepared within the potential range (-0.28 to -0.60 V) where UPD of In on Pd occurs, the characteristic XRD patterns of pure Pd and In disappeared upon the formation of Pd–In alloys, indicating that solid solutions were formed. On the other hand, when the electrodeposition was conducted at even more negative potentials (<-1.0 V) where OPD of In occurs, the In content in the deposits was greatly increased so that the Pd content was reduced to 36 at.%, the XRD diffraction patterns of the deposits were complicate showing the presence of segregated Pd, In and Pd–In compounds in the electrodeposits. The formation of solid solutions in the deposits with a high Pd content and the formation of intermetallic compounds in the deposits with a low Pd content are consistent with the phase diagram of the In–Pd system [37], and had been reported also for the electrodeposition of Pd–In in aqueous bath. [5]. As also indicated in Fig. 7, the solid solution deposits exhibited a lower diffraction angle, 2θ , in comparison to that of pure Pd, indicating that the lattice parameter of the solid solution deposits was increased upon the addition of In. On the other hand, the 2θ for the electrodeposits containing In–Pd compounds shifted to higher values, suggesting that their lattice parameters were smaller than that of pure Pd. These results agree with the results reported in literature [5].

The electrodeposition behavior was also studied at lower temperatures (30 and 80 °C). The results revealed that lowering the temperature shifts the depositions of Pd and In negatively, and decreases the deposition rate by increasing the viscosity of the IL. Furthermore, decreasing the temperature decreases the interdiffusion between the electrodeposited Pd and In.

4. Summary and conclusions

The electrochemical deposition of palladium and indium in the [EMIm]Cl- BF_4 ILs was studied with cyclic voltammetry at a GC electrode at 120 °C. The OPD of Pd occurs at a potential far more positive than the OPD of In. Such a big difference in deposition potential makes it difficult to electrodeposit compact Pd–In alloys coating. Nevertheless, the underpotential deposition of In occurs on the electrodeposited Pd at a potential overlaps with the deposition of Pd. This fact makes it possible to prepare smooth and compact Pd–In coatings. Because the UPD rate of In on Pd is slow, the In content in the deposited Pd–In alloys is lower than that in the plating bath.

Acknowledgment

Funding was provided by the National Science Council of the Republic of China, Taiwan.

References

- [1] M. Schlesinger, M. Paunovic (Eds.), *Modern Electroplating*, Wiley & Sons, New York, 2000, p. 483.
- [2] A.A. Tikhonov, P.M. Vyacheslavov, G.K. Burkat, *Zh. Prikl. Khim.* 54 (1981) 364.
- [3] F.M. Dzhandubaeva, G.K. Burkat, P.M. Vyacheslavov, *Zh. Prikl. Khim.* 54 (1981) 2331.
- [4] F.M. Dzhandubaeva, G.K. Burkat, P.M. Vyacheslavov, *Zh. Prikl. Khim.* 54 (1981) 2334.
- [5] N.F. Reshetnikova, K.S. Pedan, *Zh. Prikl. Khim.* 55 (1982) 1996.
- [6] P.M. Vyacheslavov, G.K. Burkat, A.A. Tikhonov, F.M. Dzhandubaeva, *Zh. Prikl. Khim.* 63 (1990) 436.
- [7] C.L. Hussey, J.S. Wilkes, in: A.I. Mamantov, Popov (Eds.), *Chemistry of Nonaqueous Solutions*, Current Progress, VCH, New York, 1994, p. 227.
- [8] G.R. Stafford, C.L. Hussey, in: D.M. Alkire, Kolb (Eds.), *Advances in Electrochemical Science and Engineering*, vol. 7, Wiley-VCH, 2001, p. 275.
- [9] F. Endres, *Chem. Phys. Chem.* 3 (2002) 144.
- [10] M.C. Buzzeo, R.G. Evans, R.G. Compoton, *Chem. Phys. Chem.* 5 (2004) 1106.
- [11] J. Sun, D.R. MacFarlane, M. Forsyth, *Solid State Ionics* 147 (2000) 333.
- [12] C. Tiyaipiboonchaiya, J.M. Pringle, D.R. MacFarlane, M. Forsyth, J. Sun, *Macromol. Chem. Phys.* 204 (2003) 2147.
- [13] M. Doyle, S.K. Choi, G. Proulx, *J. Electrochem. Soc.* 147 (2000) 34.
- [14] R.F. de Souza, J.C. Padilha, R.S. Goncalves, J. Dupont, *Electrochem. Commun.* 5 (2003) 728.
- [15] T. Welton, *Chem. Rev.* 99 (1999) 2071.
- [16] R.D. Rogers, K.R. Seddon (Eds.), *Ionic Liquids: Industrial Applications to Green Chemistry*, ACS, Washington, DC, 2002.
- [17] P. Wasserscheid, T. Welton (Eds.), *Ionic Liquids in Synthesis*, Wiley-VCH, Weinheim, 2002.
- [18] R.D. Rogers, K.R. Seddon (Eds.), *Ionic Liquids as Green Solvents: Progress and Prospects*, ACS, Washington, DC, 2003.
- [19] (a) J.D. Holbery, K.R. Seddon, *Clean Prod. Processes* 1 (1999) 233; (b) P. Wasserscheid, W. Keim, *Angew. Chem. Int. Ed.* 39 (2000) 3773.

- [20] C.J. Adams, M.J. Earle, K.R. Seddon, *Green Chem.* (2000) 21.
- [21] P. Lozano, T. De Diego, D. Carrie, M. Vaultier, J.L. Iborra, *J. Mol. Catal. B* 21 (2003) 9.
- [22] S. Dai, Y.H. Ju, C.E. Barns, *J. Chem. Soc., Dalton Trans.* (1999) 1201.
- [23] E.G. Yanes, S.R. Gratz, M.J. Baldwin, S.E. Robison, A.M. Stalcup, *Anal. Chem.* 73 (2001) 3838.
- [24] J.L. Anderson, D.W. Armstrong, *Anal. Chem.* 75 (2003) 4851.
- [25] (a) P.-Y. Chen, I.-W. Sun, *Electrochim. Acta* 45 (1999) 441;
(b) P.-Y. Chen, I.-W. Sun, *Electrochim. Acta* 45 (2000) 3163;
(c) M.-H. Yang, I.-W. Sun, *J. Appl. Electrochem.* 33 (2003) 1077.
- [26] Y. Katayama, S. Dan, T. Miura, T. Kishi, *J. Electrochem. Soc.* 148 (2001) C102.
- [27] (a) F. Endres, *Phys. Chem. Chem. Phys.* 3 (2001) 3165;
(b) F. Endres, M. Bukowski, R. Hempelmann, H. Natter, *Angew. Chem. Int. Ed.* 42 (2003) 3428;
(c) F. Endres, S.Z. El Abedin, *Phys. Chem. Chem. Phys.* 4 (2002) 1640;
(d) S.Z. El Abedin, N. Borissenko, F. Endres, *Electrochem. Commun.* 6 (2004) 510.
- [28] I. Mukhopadhyay, W. Freyland, *Langmuir* 19 (2003) 1951.
- [29] R.F. de Souza, J.C. Padilha, R.S. Goncalves, *Electrochem. Commun.* 5 (2003) 728.
- [30] P. He, H. Liu, Z. Li, Y. Liu, X. Xu, J. Li, *Langmuir* 20 (2004) 10260.
- [31] I.-W. Sun, C.L. Hussey, *J. Electroanal. Chem.* 274 (1989) 325.
- [32] H.C. De Long, J.S. Wilkes, R.T. Carlin, *J. Electrochem. Soc.* 141 (1994) 1000.
- [33] F.-Y. Su, J.-F. Huang, I.-W. Sun, *J. Electrochem. Soc.* 151 (2004) 811.
- [34] J.S. Wilkes, J.A. Levisky, R.A. Wilson, C.L. Hussey, *Inorg. Chem.* 21 (1982) 1263.
- [35] (a) J.S.-Y. Liu, I.-W. Sun, *J. Electrochem. Soc.* 144 (1997) 140;
(b) M.-H. Yang, I.-W. Sun, *J. Chin. Chem. Soc.* 51 (2004) 253.
- [36] (a) D.M. Kolb, M. Przasnyski, H. Gerischer, *J. Electroanal. Chem.* 54 (1974) 25;
(b) E. Budevski, G. Staikov, W.J. Lorenz, *Electrochemical Phase Formation and Growth*, VCH, New York, 1996 (Chapter 3);
(c) H.B. Michaelson, in: R.C., Weast (Ed.), *Handbook of Chemistry and Physics*, CRC Press, Boca Raton, FL, 1984–1985, p. E76.
- [37] T.B. Massalski, *Binary Alloy Phase Diagrams*, American Society for Metals, Metals Park, OH, 1986.